# Alternative Splicing Involving the Thioredoxin Reductase Module in Mammals: A Glutaredoxin-Containing Thioredoxin Reductase 1†

Dan Su and Vadim N. Gladyshev*

*Department of Biochemistry, University of Nebraska−Lincoln, Lincoln, Nebraska 68588*

*Received January 2, 2004; Revised Manuscript Received July 16, 2004*

ABSTRACT: Thioredoxin reductase 1 (TR1) is a key component in the thioredoxin system, one of major redox systems in mammals that links NADPH and thiol-dependent processes. Mammalian TR1 genes are known to be regulated by alternative splicing. In this report, comparative genomic analyses were used to identify and characterize species-specific and common alternative forms of mammalian TR1 genes. Six human TR1 isoforms were identified that were derived from a large number of transcripts and differed in their N-terminal sequences. One isoform resulted from exons located 30−70 kb upstream of the previously identified core TR1 promoter and was composed of a basic TR1 module fused to a glutaredoxin (Grx) domain that contained an unusual active site CTRC sequence. This TR1 form occurred in humans, dogs, and chimpanzees but was inactivated in mice and rats. The CTRC motif in the human enzyme made the N-terminal domain inactive in the Grx assays tested. However, when mutated to CPYC, an active site present in most Grxs, the Grx domain was active. In addition, the presence of the Grx domain interfered with the TR1 activity, distinguishing this enzyme from other proteins with Grx and TR fusions. The data suggest that the fusion of the basic TR1 module and variable N-terminal sequences links the pyridine nucleotide thiol/disulfide oxidoreductase pathway to specific cellular redox functions and may control spatial and temporal expression of TR1 transcripts. Our data also suggest that various N-terminal extensions in mammalian TRs are often expressed in testes.

The thioredoxin (Trx)[1] system is one of two major redox systems in cells (*1*, *2*). It is composed of thioredoxin reductase (TR), Trx, and thioredoxin peroxidase and is present in all organisms. In this system, a small thiol/disulfide oxidoreductase Trx and Trx peroxidase (also called peroxiredoxin) are two Trx-fold proteins that use cysteine chemistry for redox reactions. The reduced state of Trx is maintained by TR, which is an NADPH-dependent FAD-containing enzyme and a member of the pyridine nucleotide disulfide oxidoreductase family (*3*). There are two known TR types that evolved by convergent evolution (*4*, *5*): a homodimer of 35 kDa subunits present in prokaryotes, yeast, and plants (*6*) and a homodimer of 55−65 kDa subunits that occurs in animals and some lower eukaryotes (*2*, *7*, *8*).

Mammalian TRs are selenoproteins with a penultimate selenocysteine (Sec) in its carboxyl-terminal active center (*9*, *10*). TR plays a central role in reduction of disulfides and other oxidized forms of cysteine residues in redox-regulated proteins through its substrate Trx. TR can also reduce a broad spectrum of small molecules, such as hydroperoxides (*11*), selenite (*12*), dehydroascorbate (*13*), NK-lysin, and vitamin K. Three mammalian TR genes were previously identified that encode TR1 (cytosolic enzyme, also called TrxR1), TGR (thioredoxin and glutathione reductase, also called TR2 or TrxR3) (*7*), and TR3 (a mitochondrial TR, also called TrxR2 and TR$\beta$) (*14*−*16*). The three mammalian TRs are highly homologous and contain a conserved CVNVGC active site in the N-terminal regions and a carboxyl-terminal GCUG (U represents Sec) tetrapeptide that are both essential for TR function (*17*, *18*). TGR was found to have an additional domain with homology to glutaredoxin (Grx) (*7*). Grx is a component of another major redox system, the glutathione system (*19*).

It is generally thought that the Trx and glutathione systems function independently of each other in vivo. However, the finding of TGR suggested that these two systems may interact with each other. Moreover, it was found that *Drosophila melanogaster* does not have a functional glutathione reductase and that glutathione is reduced in this organism via the Trx system (*20*).

Following identification of the Grx-fused TGR in mammals, similarly organized homologous proteins were found in several other organisms, including three parasites (*21*−*23*), indicating that the fusion of Grx and TR domains is not limited to mammals. However, there are important differences between mammalian and parasite TGRs. First, the

† This research was supported by Grant GM065204 from the National Institutes of Health.

* To whom correspondence should be addressed. Phone: (402) 472-4948. Fax: (402) 472-7842. E-mail: vgladyshev1@unl.edu.

[1] Abbreviations: TR, thioredoxin reductase; Grx, glutaredoxin; Trx, thioredoxin; NADPH, reduced nicotinamide adenine dinucleotide phosphate; TGR, thioredoxin glutathione reductase; GSS, genome survey sequence; HTGS, high-throughput genomic sequences; WGS, whole genome shotgun; SECIS, selenocysteine insertion sequence; DTNB, 5,5′-dithiobis(2-nitrobenzoic acid); AMS, 4-acetamido-4′-maleimidylstilbene-2,2′-disulfonic acid; GSH, reduced glutathione; GSSG, oxidized glutathione; EDTA, ethylenediaminetetraacetic acid; SDS−PAGE, polyacrylamide gel electrophoresis in the presence of sodium dodecyl sulfate; GR, glutathione reductase; BLAST, basic local alignment search tool; Tris, tris(2-aminoethyl)amine; EST, expressed sequence tag.

10.1021/bi048478t CCC: $27.50 
Published on Web 08/31/2004

mammalian enzyme has a tissue-specific expression pattern; the protein is almost exclusively expressed in testis (unpublished data); and second, the Grx domain of mammalian TGR contains a CxxS (cysteine separated from serine by two other residues) active site motif, whereas the parasite TGRs contain a typical CxxC active site motif that is found in most glutaredoxins (*21*−*23*). These differences suggest that, despite similar domain organization, mammalian and parasite TGRs may represent two functionally distinct types of proteins.

Analysis of TR1 mRNA expression revealed its low levels in brain and high levels in the medullary rays of the rat kidney (*24*). Interestingly, a kidney-derived cDNA clone differed from known TR1 cDNA sequences in 5′ sequences (*24*). In addition, a third differential 5′ sequence was detected in rodents. We also observed three differential 5′ sequences in rodent TR1 genes and predicted that they result from alternative first exon splicing (*25*). It was also proposed that alternative splicing could explain, at least in part, extensive heterogeneity within human TR1 preparations. However, genomic sequences of any of the TR1 genes were not available to test these predictions. After completion of human and mouse genomic projects, the three alternative cDNA forms were mapped to genomic sequences, providing further support for regulation of TR1 by alternative splicing (*26*).

In this report, we used comparative genomic methods to map available mammalian TR1 cDNA sequences and identified novel, species-specific and common alternatively spliced forms of this protein. Analysis of these forms revealed that the basic TR1 module is fused to various redox sequences and that such fusion allows the linkage of these sequences to an electron donor, NADPH, and provides expression of the fusion proteins in temporal and spatial manner. Surprisingly, we also identified a Grx domain-containing form of TR1. This form exists in human, chimpanzee, and dog but is inactive in mouse and rat.

## EXPERIMENTAL PROCEDURES

*Materials*. All chemicals were obtained from Sigma unless indicated otherwise. Competent cells were obtained from Novagen.

*Sequence Analysis*. Sequence analyses were performed using various *b*asic *l*ocal *a*lignment *s*earch *t*ool (BLAST) programs (http://www.ncbi.nlm.nih.gov/BLAST/) and various NCBI databases [nonredundant (NR), database of expressed sequence tags (dbEST), Genome Survey Sequence (GSS), High Throughput Genomic Sequences (HTGS), and Whole Genome Shotgun (WGS)]. SECIS element prediction was performed using SECISearch 2.0 (http://genomics.unl.edu/SECISearch.html) (*27*). The presence of signal peptides was assessed by PSORT II (http://psort.ims.u-tokyo.ac.jp/form2.html), SignalP (http://www.cbs.dtu.dk/services/SignalP-2.0/), Signal Peptide Prediction (http://bioinformatics.leeds.ac.uk/prot_analysis/Signal.html), and Mitoprot (http://ihg.gsf.de/ihg/mitoprot.html). Multiple sequence alignment was performed using ClustalW (*28*) in BioEdit, and the alignment figures were generated in BioEdit. Phylogenetic analyses were performed using PHYLIP. Tissue- and cell-type information of various ESTs (Supporting Information, Table S3) was retrieved from the NCBI EST database.

*Construct Preparation.* 5′-GAGTATTCATATGGGCTGCGCCGAGGGCAAGGCA-3′ was used as the 5′ primer to amplify various Grx-TR1 forms and the Grx domain sequences from an EST clone BG772375. 5′-GCGAAGCTTCATCCACACTGGGGCTTAACCTCAGCA-3′ was used as the 3′ primer to amplify the truncated form of Grx-TR1. 5′-GCGAAGCTTCATCCACACTGGGGCTTAACCGCAGCA-3′ was used as the 3′ primer to amplify the cysteine mutant of Grx-TR1. 5′-TATAAGCTTAGCTAGCGATTGGTGCAGACCTGCAACCGATGGACCTCAGCAGCCAGCCTGGAGGATGC-3′ was used as the 3′ primer to amplify the wild-type Grx-TR1 form. These sequences contained an *Escherichia coli* formate dehydrogenase H SECIS element immediately downstream of the stop signal. The PCR products of the above three constructs were inserted into the pET28a vector (Novagen) between *Nde*I and *Hin*dIII sites. When expressed, these constructs generated proteins containing N-terminal 6-His tags.

5′-TATAAGCTTAGCTAGCGATTGGTGCAGACCTGCAACCGATGGTTAACCTCAGCAGCCAGCCTGGAGGATGC-3′ was used as the 3′ primer to amplify the tagged wild-type Grx-TR1 form. An *E. coli* formate dehydrogenase H SECIS element was also present in this construct followed by a sequence coding for a C-terminal 6-His tag. The PCR product was inserted into the pET21b vector (Novagen) between *Nde*I and *Hin*dIII sites.

The preparation of TR1 constructs was similar to that of Grx-TR1, except that 5′-GAGTATTCATATGAACGGCCCTGAAGATCTTCCC-3′ was used as a 5′ primer. 5′-GAGTATTCATATGGGCTGCGCCGAGGGCAAGGCA-3′ and 5′-GCGAAGCTTATTTTAGTAGCTTTTGAAG-3′ were used to amplify the Grx domain. Point mutations were obtained using the QuickChange XL site-directed mutagenesis kit from Stratagene according to the protocol of the manufacturer.

*Expression.* Recombinant proteins were expressed in the BL21(DE3) strain (Novagen), and His-tagged proteins were purified using Ni-NTA−agarose (Qiagen) according to the QIAexpressionist protocol (Qiagen).

*Analysis of Redox Potential.* To determine the redox potential of the Grx domain, a previously reported method (*29*) was used. Briefly, 15 $\mu$g of the recombinant mutant Grx domain (C3S/C90S) was incubated in 100 mM sodium phosphate, pH 7.0, and 1 mM EDTA redox buffer in the presence of variable GSH/GSSG concentrations and ratios at room temperature for 4 h. The GSH content was determined by titration using 5,5′-dithiobis(2-nitrobenzoic acid) (DTNB) before and after the incubation ($\epsilon_{412} = 13600$ $M^{-1}$ $cm^{-1}$). Ice-cold TCA (15%) was added to all samples, and samples were incubated on ice for 15 min. The precipitated proteins were then spun down by centrifugation at 13000 rpm for 10 min, and the precipitates were washed with ice-cold acetone and recentrifuged. The tubes were dried and the proteins resuspended in 9 $\mu$L of 100 mM sodium phosphate, pH 7.0, 1 mM EDTA, and 1% SDS, followed by addition of 15 mM 4-acetamido-4′-maleimidylstilbene-2,2′-disulfonic acid (AMS; Molecular Probes) to the samples. The alkylation was performed at 37 °C for 2 h, and the samples were subjected to SDS−PAGE under nonreducing conditions and Coomassie Blue staining. The redox potential was calculated as described (*30*).

*$^{75}$Se Labeling.* Five milliliters of *E. coli* cells carrying the tagged TR1 plasmid were grown to $OD_{600}$ 0.6, and 0.08 mCi of freshly neutralized $^{75}$Se[selenite] was added along with

0.1 mM IPTG to the cell culture. Cells were grown for 12 h at 30 °C, collected by centrifugation, and solubilized in SDS−PAGE sample buffer, and proteins were electrophoresed and transferred to a PVDF membrane. The membrane was exposed for 12 h, and the $^{75}$Se radioactivity pattern was visualized using a PhosphorImager. The membrane was also subjected to western blot analysis using anti-His-tag antibodies (Novagen).

*Enzyme Assays.* Thioredoxin reductase activities were assayed using two methods: (i) NADPH-dependent reduction of DTNB determined as an increase in absorbance at 412 nm at 25 °C (*31*). A reaction mixture contained 0.2 mM NADPH, 5 mM DTNB, and 10 mM EDTA in 0.5 mL of 100 mM sodium phosphate buffer, pH 7.0. Recombinant protein (200 $\mu$M) was used in each activity measurement. The activity was calculated as $[(OD_{412} \times 0.5\ mL)/(13.6\ mmol \times 2)] \times 60\ s\ min^{-1}$ (mg of protein)$^{-1}$. (ii) NADPH-dependent reduction of 0.5 mg/mL insulin and 3 $\mu$M *E. coli* Trx was determined as a decrease in absorbance at 340 nm at 25 °C (*31*). The reaction mixture contained 0.2 mM NADPH, 0.5 mg/mL insulin, 1 mM EDTA, and 3 $\mu$M Trx in 0.5 mL of 50 mM phosphate buffer, pH 7.0. The activity was calculated as $[(OD_{340} \times 0.5\ mL)/(6.22\ mmol)] \times 60\ s\ min^{-1}$ (mg of protein)$^{-1}$.

Glutathione reductase activity was assayed as the NADPH-dependent reduction of GSSG determined as the decrease in absorbance at 340 nm at 25 °C (*32*). The 0.5 mL reaction solution contained 0.2 mM NADPH, 5 mM GSSG, and 1 mM EDTA in 100 mM Tris-HCl, pH 7.6. One unit of GR reduces 1 $\mu$mol of oxidized GSSG/min.

Grx activity was assayed as the decrease in absorption at 340 nm at 25 °C (*19*). The reaction mixture contained 0.2 mM NADPH, 1 mM GSH, 2 mM EDTA, 0.4 unit of GR, and 1 mM $\beta$-hydroxyethyl disulfide (HED) in 0.5 mL of 0.1 M Tris-HCl buffer, pH 8.0. The Grx sample was added to the solution after 2 min of incubation. One unit of activity was defined as the consumption of 1 $\mu$mol of NADPH/min.

Disulfide bond isomerization activity was assayed as the activation of denatured RNase A (sRNase A), a fully oxidized protein containing predominantly nonnative disulfides. Only those RNase A molecules possessing all four native disulfides have significant ribonucleolytic activity. sRNase A was obtained as described in Woycechowsky et al. (*33*). Briefly, fully reduced RNase A (70 $\mu$M) in 20 mM Tris-HCl buffer, pH 8.0, containing 6 M guanidine hydrochloride and 1 mM EDTA was fully oxidized by air and diamide, the reducing agent was removed by running a PD-10 column (Amersham Biosciences, Piscataway, NJ) in the presence of 6 M guanidine hydrochloride, then 5 mM diamide was added to the protein, and the solution was incubated at 37 °C for 2 h. Exhaustive dialysis against 0.1 M Tris-HCl buffer, pH 7.6, containing 1.0 mM EDTA was then performed to remove guanidine hydrochloride. This method produced RNase A with <0.1 mol of thiol/mol of protein and approximately 1% of the ribonucleolytic activity of native RNase A. The RNase A activity was determined by following the hydrolysis of 2′,3′-cCMP as an increase in absorbance at 296 nm ($\Delta\epsilon_{296} = 0.19\ mM^{-1}$). cCMP (5 mM) was incubated with 1 $\mu$M sRNase A and the recombinant Grx domain for up to 1 h. The differences in absorbance at 296 nm were determined at different times and used to calculate RNase A activity. Native RNase A was used as the positive control.

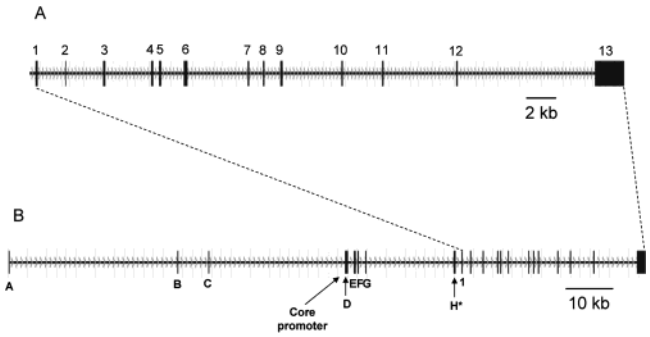


FIGURE 1: Genomic organization of the human TR1 gene. (A) Core exons in the human TR1 gene are shown by vertical lines and boxes and are numbered from 1 to 13. (B) All exons in the human TR1 gene. Alternatively spliced exons are designated by letters from A to H with exons A to G supported by the presence of cDNA sequences and exon H predicted by comparative genomic methods. The position of the core promoter is indicated in (B).

*Western Blotting.* Polyclonal antibodies against the recombinant Grx domain of human TR1 were generated by Covance (Princeton, NJ). The antibodies were further purified on an affinity column containing the recombinant Grx domain. Immunoblot assays were performed using standard procedures at 1:1000 dilution of primary antibodies. Membranes were developed using an ECL system (Amersham Biosciences. Piscataway, NJ).

## RESULTS AND DISCUSSION

Human and mouse TR1 genes are known to be alternatively spliced (*24*−*26*), but alternative splicing forms have not been previously characterized. Our initial sequence analyses revealed that the number of alternative cDNA forms is much larger than the three previously identified, and these encode differential N-terminal sequences in TR1. Therefore, we performed an exhaustive search for such forms expressed from mammalian TR1 genes.

*Human TR1 Gene.* We mapped the EST and nonredundant sequences that were homologous to previously identified human TR1 cDNA forms to human genomic sequences and analyzed genomic structures of detected alternative forms. The coding region of TR1 spans 13 core exons on chromosome 12, with the first exon containing the AUG start codon and the last exon the Sec-coding TGA codon and SECIS element. We designate these core exons as exons 1−13 (Figure 1A). We could find no evidence for functional exon deletion, insertion, or alternative splicing within these 13 exons. We thus focused on additional exons upstream of exon 1.

We detected sequences for nine alternatively spliced forms that contained additional exons (Figure 2, forms 2−10) and were supported by the presence of cDNA sequences. Together with the form that started with exon 1 (Figure 2, form 1) there were total of ten splicing forms. These ten forms involved seven additional exons, which we designated as exons A−G (Figure 1B). Among the seven exons, exon D was spliced at different 3′ splicing sites. The relative size and position of all exons, as mapped on the genomic sequence, are shown in Figure 1B.

The ten splicing forms and an additional predicted form (see below) coded for six TR1 ORFs that differed in their N-terminal regions (Supporting Information, Tables S1 and S2). We designated these as isoforms I−VI. Isoform I, which

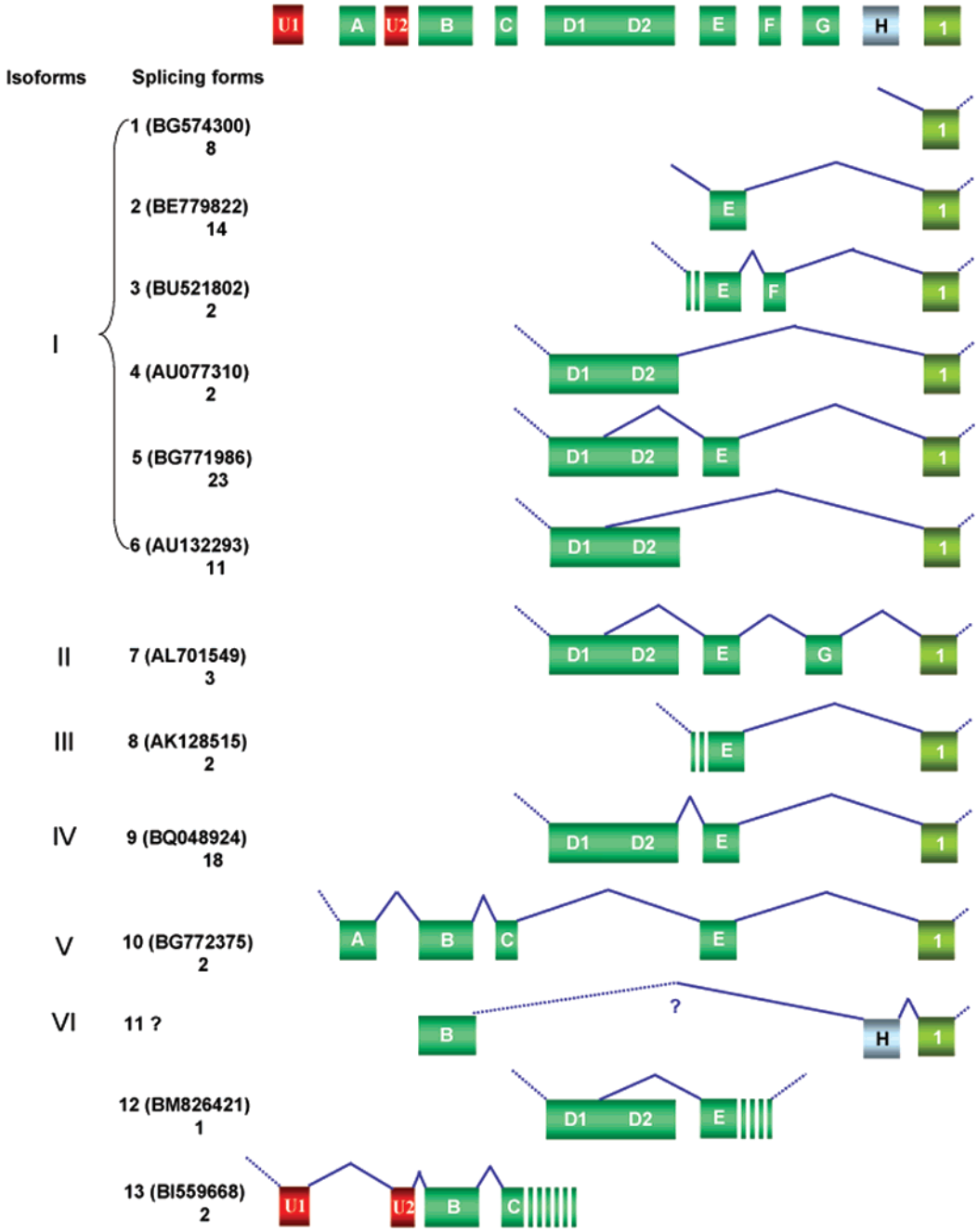


FIGURE 2: Alternatively spliced forms of the human TR1 gene. A representative EST entry is given for each splicing form, and the total number of ESTs corresponding to each form is shown below the accession number. Splicing form 11 is predicted by comparing mouse, rat, and human TR1 genes. No human ESTs are available for this form. Exons U1 and U2 are also shown, but these do not result in TR1 coding regions. Some exons did not splice at typical splice sites; EST sequences revealed that these exons extended beyond predicted splice sites (indicated by dashed exon segments in the figure).

was the major TR1 form, was represented by cDNA forms 1−6 (Figure 2 and Supporting Information, Tables S1 and S2). Translation of all six isoforms was predicted to start from the ATG codon that was located in exon 1, encoding a 499 amino acid ORF, which we designated as a basic TR1 module (Supporting Information, Tables S1 and S2).

Isoform II was encoded by splicing form 7, which was represented by three ESTs and was the only form that contained exon G. This isoform contained 44 additional amino acid residues at the N-terminus of TR1, MLSRLVLNSWAQAIIRPRPPKVLGLQVTTFSEAYQEGRLQKLLK. PSORT II predicted that this sequence had a mitochondrial targeting signal, whereas SignalP and other prediction methods made no such prediction. A tBLASTn search against various sequence databases revealed conserved sequences in mouse, *Drosophila*, and chimpanzee. However, the N-terminal extension was also homologous to Alu repeats. Further studies are needed to establish whether this isoform is functional.

Isoform III was represented by splicing form 8 and coded for 99 N-terminal amino acids upstream of the basic TR1 module, MQQVMLTCKGVNRGHAVPAGPGRKPRPRRSSRLLAGEKHLTRSALLLCHTEDGRALEGTLSELAAETDLPVVFVKQRKIGGHGPTLKAYQEGRLQKLLK. This

isoform was generated due to lack of exon G compared to splice variants coding for isoform I. We could not find any homologues of this sequence in other mammalian genomes or cDNA sequence databases. This sequence contained a putative glutathione binding site present in Grx sequences but lacked an N-terminal active site of such proteins.

Isoform IV was represented by splicing form 9 and coded for an additional 52 amino acids, MSCEDGRALEGTLSELAAETDLPVVFVKQRKIGGHGPTLKAYQEGRLQKLLK, at the N-terminus of the basic TR module, due to the presence of exon E. This sequence also contained the C-terminal part of the Grx domain, including the putative glutathione binding site. However, the lack of N-terminal sequences within the Grx domain would preclude it from forming the Trx fold.

Isoform V was represented by splicing form 10. Two ESTs (BG772375 and BG717223) corresponded to this splicing form. We generated a full cDNA sequence of BG772375 and determined that there was a sequence error within the NCBI sequence, which caused a frame shift. The correct cDNA sequence coded for a protein with an N-terminal 150 amino acid extension relative to the basic TR1 module. Conserved domain and PSI-Blast searches indicated that this extension corresponded to a Grx domain and identified a conserved CxxC active site motif within the N-terminal part of the domain. Further phylogenetic analyses using a large collection of Grx sequences revealed that the Grx domain in TR1 clustered with the Grx domain found in TGR and with a *Danio rerio* TR1 sequence, which also contained the Grx domain (Figure 3A).

We further aligned an entire amino acid sequence of the human Grx-containing TR1 isoform (Grx-TR1) with available TGR and fish TR1 sequences. The sequence alignment (Figure 3B) revealed that all of these proteins contained a conserved Grx domain with either CxxC or CxxS motifs and a basic TR module with the conserved CVNVGC active site and a C-terminal GCUG tetrapeptide. The phylogenetic tree generated using the full-length sequences (Figure 3C) was organized similarly to that generated using Grx sequences (Figure 3A). These analyses showed that the human Grx-TR1 form was evolutionarily closer to *D. rerio* TR1 and mammalian TGRs than to *Echinococcus granulosus* and *Schistosoma mansoni* TGRs. Thus, the data suggested that these proteins evolved from a common ancient ancestor, in which the Grx domain and the TR module were fused. It also appears that the CxxC motif was the initial sequence in the ancestor TR-fused Grx domain and that it gave rise to the CxxS motif in mammalian TGRs.

Besides the ten alternatively spliced forms, there were at least two additional forms that were generated by exon splicing but terminated upstream of the sequences coding for the basic TR1 module. Splicing form 12 was not spliced at the 3′ splicing site of exon E and contained genomic sequences downstream of exon E. It is possible that this form was generated from an erroneous pre-mRNA.

Splicing form 13 contained two additional exons, U1 and U2, which could not be found in any other alternatively spliced forms of the human TR1 gene, and exons B and C. This form was the only other alternative form that contained exons B and C other than form 10. Similarly to form 12, form 13 did not splice at the 3′ splicing site of exon C and was further extended along the genomic sequence. Finally, a splicing form (form 11) was predicted that coded for isoform VI but was not represented by available human cDNA sequences (described below). Tissue distribution of alternatively spliced forms, determined by analyzing human ESTs, is shown in Table S3 (see Supporting Information).

*Mouse and Rat TR1 Genes.* The TR1 gene was located on chromosome 10 in the mouse genome and chromosome 7 in the rat genome. As in the human gene, the basic TR1 module was encoded by exons 1−13. The exhaustive analysis of mouse EST and nonredundant sequences revealed that the mouse TR1 gene also had alternative exons D and E. On the other hand, no cDNA sequences could be detected to support the occurrence of mouse exons F and G. There was an additional alternatively spliced form, which was not detected by mapping human cDNA sequences on the human genome. This form encoded a 102 amino acid N-terminal extension in the mouse TR1 (*25*). PSI-Blast and conserved domain searches revealed no homology to known domains. However, like the Grx form of human TR1, this form had a CxxC sequence, suggesting a possible redox function.

Mapping of this form to the mouse genomic sequence revealed two additional exons upstream of exon 1. To further analyze this splicing form, we analyzed the two mouse exons against the human TR1 genomic and cDNA sequences. By comparing relative positions and sequence conservation of the first of these two exons, we found that it was homologous to human exon B (Figure 4A). In addition, when the mouse genomic region containing the two exons was analyzed by BLAST against the corresponding human genomic region, the human counterpart of both mouse exons could easily be observed (Figure 4C). Using the same method, we also found the rat counterparts of both exons (Figure 4C). Mouse and rat sequences exhibited 69% identity to human exon B, suggesting a common evolutionary origin. Furthermore, sequence analysis of the dog shotgun genome revealed the two conserved exons (accession number AACN010048775). The conservation of these exons and protein sequences encoded by them (Figure 4D) suggests that this rare form is present in various mammals, including humans, even though no human cDNA sequences could be detected in sequence databases. Thus, an additional alternatively spliced form, human form 11 that coded for isoform VI, could be predicted in the human TR1 gene (Figure 2). Phylogenetic analysis (Figure 3C) showed that the human protein was closer to the dog sequence than to those of mouse and rat.

Identification of the alternatively spliced human form 11 using mouse, rat, and dog sequences raised the question of whether a mouse cDNA form can be detected that encoded Grx-TR1. Analysis of mouse cDNA sequences revealed no ESTs that corresponded to human exons A or C, but exon B was present in the mouse form described above. We analyzed human exon A and C sequences against mouse and rat genomic sequences but failed to identify homologous sequences. In the pairwise comparison of human, mouse, and rat exons B (Figure 4A), we found a gap (shown by the red closed box, Figure 4A) in mouse and rat exon B sequences, which corresponded to the region coding for the CxxC motif. Thus, mouse and rat genomes lacked sequences coding for active site residues in the Grx domain. Further analysis of possible coding sequences in this exon (Figure 4B) revealed that exon B in mouse and rat genomes had several translation stop signals within the sequence. The presence of detectable

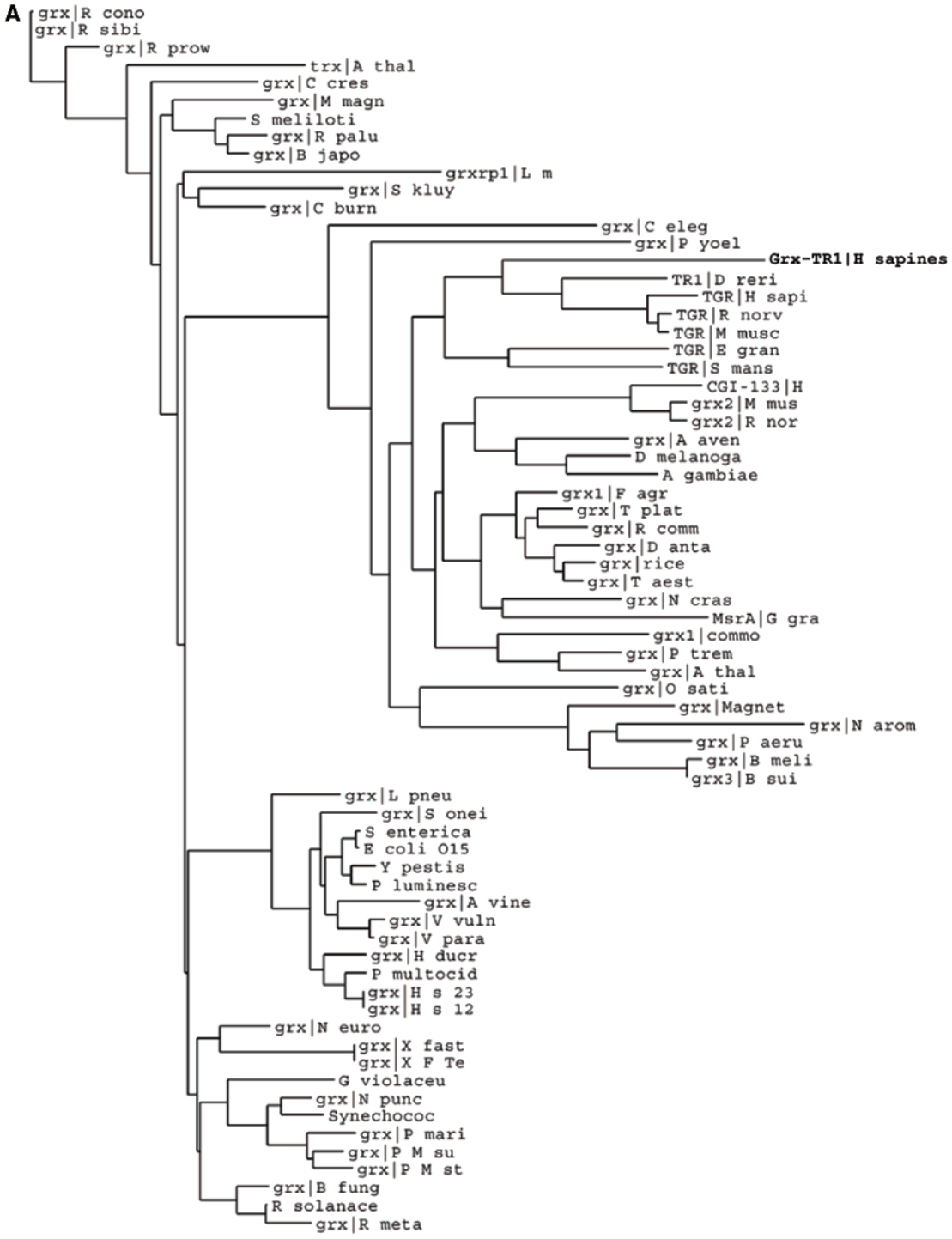
A
grx|R cono
grx|R sibi
grx|R prow
trx|A thal
grx|C cres
grx|M magn
S meliloti
grx|R palu
grx|B japo
grxrp1|L m
grx|S kluy
grx|C burn
grx|C eleg
grx|P yoel
Grx-TR1|H sapines
TR1|D reri
TGR|H sapi
TGR|R norv
TGR|M musc
TGR|E gran
TGR|S mans
CGI-133|H
grx2|M mus
grx2|R nor
grx|A aven
D melanoga
A gambiae
grx1|F agr
grx|T plat
grx|R comm
grx|D anta
grx|rice
grx|T aest
grx|N cras
MsrA|G gra
grx1|commo
grx|P trem
grx|A thal
grx|O sati
grx|Magnet
grx|N arom
grx|P aeru
grx|B meli
grx3|B sui
grx|L pneu
grx|S onei
S enterica
E coli O15
Y pestis
P luminesc
grx|A vine
grx|V vuln
grx|V para
grx|H ducr
P multocid
grx|H s 23
grx|H s 12
grx|N euro
grx|X fast
grx|X F Te
G violaceu
grx|N punc
Synechococ
grx|P mari
grx|P M su
grx|P M st
grx|B fung
R solanace
grx|R meta

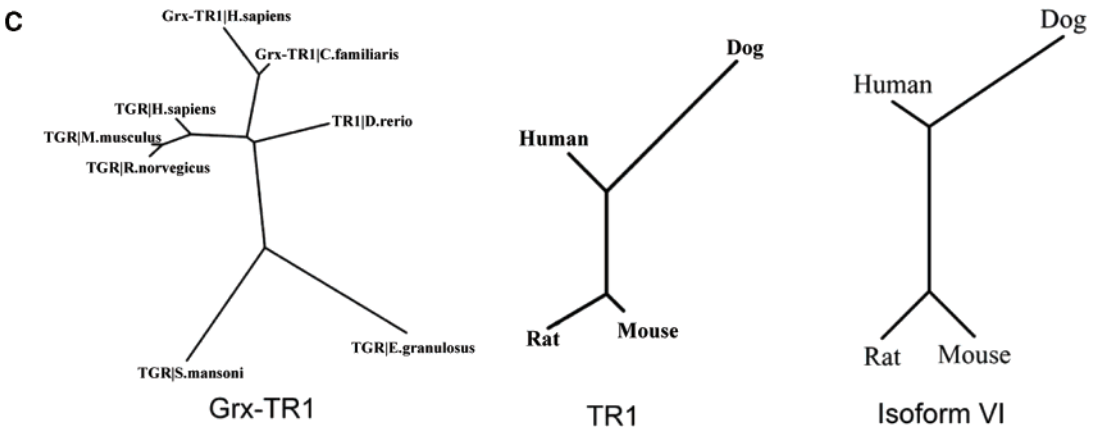
C
Grx-TR1|H.sapiens
Grx-TR1|C.familiaris
TGR|H.sapiens
TR1|D.rerio
TGR|M.musculus
TGR|R.norvegicus
TGR|E.granulosus
TGR|S.mansoni
Grx-TR1
Dog
Human
Rat
Mouse
TR1
Dog
Human
Rat
Mouse
Isoform VI

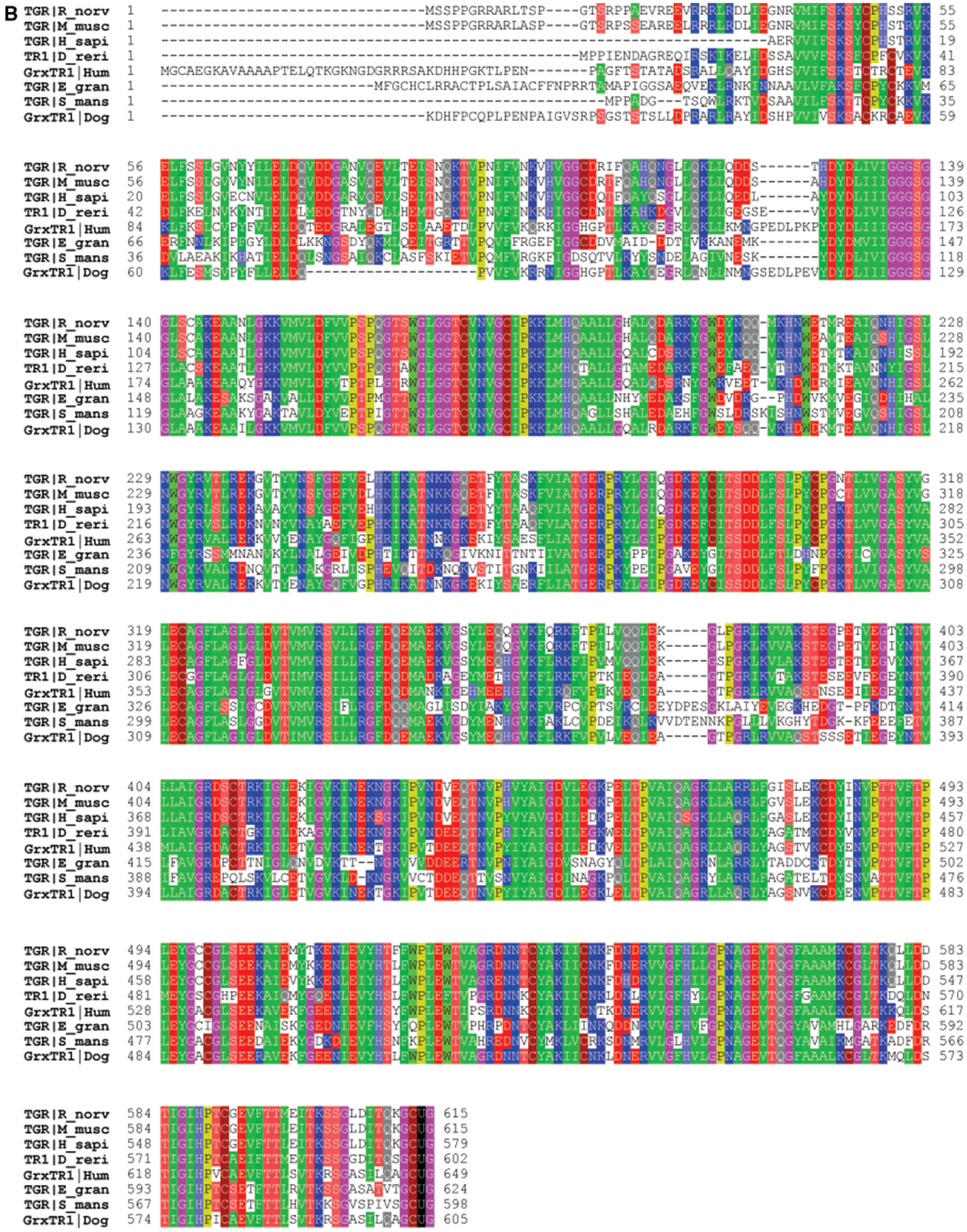


FIGURE 3: Sequence alignment and phylogenetic analysis of Grx-TR1. (A) Grx phylogenetic tree. The Grx domain of TR1 was aligned with other Grx homologues, and the phylogenetic tree was generated. (B) Sequence alignment of Grx-TR1 and its closest homologues: parasite TGRs, *D. rerio* TR1 and mammalian TGRs. (C) Phylogenetic trees of mammalian TR1. Left panel: phylogenetic tree that includes Grx-TR1|H.sapiens (human Grx-TR1), Grx-TR1|C.familiaris (dog Grx-TR1), TGR|H.sapiens (human TGR), TGR|M.musculus (mouse TGR), TGR|R.norvegicus (rat TGR), TGR|S.mansoni (*S. mansoni* TGR), TGR|E.granulosus (*E. granulosus* TGR), TR1|D.rerio (zebrafish TR1). Middle panel: phylogenetic tree of the TR1 module. Right panel: phylogenetic tree of the N-terminal sequences of isoform VI.


FIGURE 4: Homology and heterology of mammalian TR1 genes. (A) Sequence alignment of exon B in human, mouse, rat, dog, and chimpanzee genomic sequences. The exon is shown by a black closed box, and the red closed box indicates the region encoding the CxxC active site. (B) ORF view of mammalian exons B. Protein sequences were aligned according to nucleotide sequence shown in (A). Mouse and rat sequences contained in-frame stop signals, so their downstream sequences are not shown. The closed box indicates the CxxC active site. (C) Sequence alignment of exon H in the mouse TR1 gene and corresponding genomic sequences in human and rat genomes (the overall sequence identity of this exon, shown by a black box, was 69%). (D) Protein sequence alignment of the N-terminal domain of mouse isoform VI and predicted rat, human, and dog counterparts. The alignment shows 39% sequence identity.

but dysfunctional exon B in mouse and rat sequences suggested that this form was previously present but is currently inactivated in these organisms.

Is Grx-TR1 unique in humans? We analyzed the human sequences corresponding to the Grx domain against all currently available mammalian genomic sequences. A dog entry (accession number AACN010115548) was found in WGS and a chimpanzee entry (accession number AG058691) was found in the GSS database. The alignment of nucleic acid sequences within exon B (Figure 4A) and dog and chimpanzee ORFs (Figure 4B) suggested that the Grx-containing TR1 was encoded in dog and chimpanzee genomes. Further searches with human exons A and C revealed no homologous exon A sequences in mammals but found a dog exon C sequence in WGS (accession number AACN010522948). The lack of exons A and C in chimpanzee sequences was probably due to the small number of genomic sequences currently available for this animal.

To test for the occurrence of the Grx-TR1 form in vivo, we homogenized dog and bovine testis samples and applied them to an ADP−Sepharose, which is an affinity column for thioredoxin reductase and other pyridine nucleotide disulfide oxidoreductases. The enriched TR fraction was probed in immunoblot assays with antibodies developed

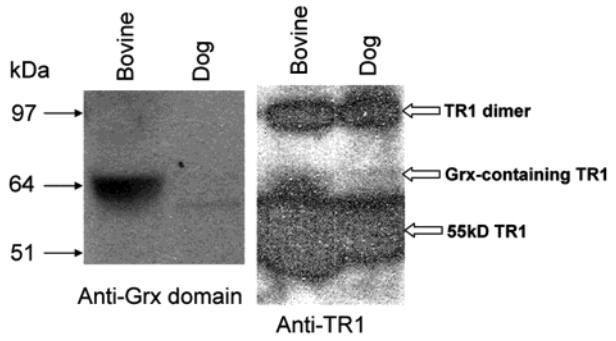


FIGURE 5: Expression of the Grx-TR1 form. Dog and bovine testes were homogenized, the extracts were fractionated on an ADP−Sepharose column, and the eluate was subjected to immunoblot assays using antibodies specific for either the Grx domain of human TR1 (left panel) or the C-terminal peptide of human TR1 (right panel). The location of the 55 kDa form (a major form of TR1) and the 67 kDa form is shown.

against the Grx domain of human TR1. A band was detected in the bovine sample that corresponded to the predicted size of the Grx-containing form (Figure 5, left panel), suggesting the presence of Grx-TR1 in the sample. The bovine and dog samples were also probed with antibodies raised against a synthetic peptide corresponding to the C-terminal 16 residues of human TR1, which detected a weak band of the 67 kDa TR1 protein in addition to a strong band of the major form of TR1 that migrated as a 55 kDa protein. It is possible that the bovine Grx-TR1 is more abundant than the corresponding dog enzyme; however, both are likely expressed at very low levels, consistent with a small number of ESTs available for this form (see below). The confirmation of the occurrence of the bovine Grx-TR1 isoform requires genomic sequences of exons A, B, and C, which are currently not available.

*Linkage of the Basic TR Module to Variable N-Terminal Sequences in Testis.* The human Grx-TR1 isoform (isoform V) was represented by two ESTs, whereas the cDNA form that contained exons U1, U2, and B was represented by three ESTs, with all five ESTs being of the testis origin. In addition, the 67 kDa mouse TR1 isoform (isoform VI) was primarily expressed in testes as previously found using real-time PCR (*34*). Thus, all forms that contained exon B appeared to be expressed in a testis-specific manner. Interestingly, the mouse TGR is highly abundant in testes (Sun, Su, Novoselov, and Gladyshev, unpublished data). Thus, it appears that the basic TR module in Grx-TR1 and TGR was linked to variable N-terminal redox domains, which were specifically expressed in testes.

Modeling of the TGR structure suggested that electrons are transferred by this enzyme from NADPH via FAD, the CVNCGC active site, and the C-terminal GCUG to the active site cysteine in the Grx domain (*7*). Similar organization of electron flow is expected in Grx-TR1 and other Grx-containing TR forms. Whereas the structure of the N-terminal domain in isoform VI is not known, it is likely that the conserved cysteines in this domain are the ultimate acceptors for NADPH electrons that are shuttled through the basic TR1 module.

The human TR1 core promoter was previously identified (*35*), and our analysis of available EST sequences suggested that most of these sequences could indeed be generated when transcription is initiated from this promoter. Homology analyses revealed a high degree of conservation within the

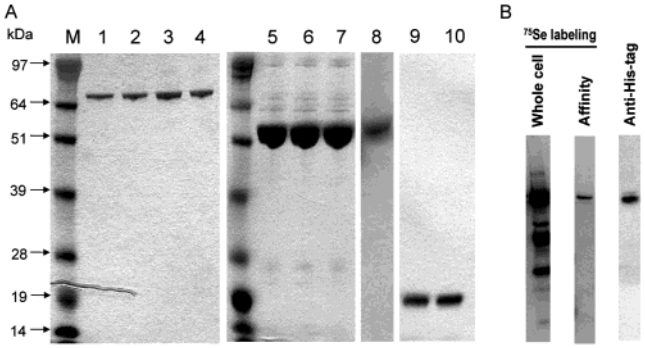


FIGURE 6: Expression of Grx-TR1 forms and their separate domains in *E. coli*. (A) Expression of TR-Grx domains and full-size proteins. Key: M, standards; lane 1, truncated form of Grx-TR1; lane 2, cysteine mutant of Grx-TR1; lane 3, wild-type Grx-TR1; lane 4, C-terminally tagged wild-type Grx-TR1; lane 5, truncated form of TR1; lane 6, cysteine mutant of TR1; lane 7, wild-type TR1; lane 8, C-terminally tagged wild-type TR1; lane 9, Grx domain; lane 10, CPYC mutant of the Grx domain. Molecular masses of standards are shown on the left. (B) $^{75}$Se labeling of the tagged TR1 form. *E. coli* cells expressing tagged TR1 were labeled with $^{75}$Se as described in Experimental Procedures. Lanes: left, crude extract; middle, protein eluted from the His-tag affinity column; right, immunoblot analysis of crude extract with anti-His-tag antibodies. Lanes 1 and 2 show PhosphorImager detection of $^{75}$Se.

core promoter sequences among mammals (Supporting Information, Figure S1). The region immediately upstream of the transcription initiation site, in particular, is highly conserved. However, the presence of upstream exons A, B, and C that were located 30−70 kb upstream of the core promoter and that gave rise to testis-specific cDNAs argues for the presence of at least one additional promoter. This promoter should be located upstream of exon A and primarily activate transcription of the TR1 gene in a testis-specific manner. A large number of alternative 5′ sequences in TR1 also suggests that the presence of additional promoters located both upstream and downstream of the core TR1 promoter cannot be excluded.

We also analyzed SECIS elements in human, mouse, rat, dog, and *D. rerio* TR1 genes. The predicted SECIS elements (Supporting Information, Figure S2) show a very high level of conservation except for the *D. rerio* structure, which has an AU sequence instead of AA in the bulge. Such form of a SECIS element has not been previously observed.

*Expression and Characterization of Human Grx-TR1.* The fact that the Grx-TR1 isoform was not present in rat and mouse but occurred in human, dog, and chimpanzee genomes suggested that it might play a specialized function in a limited number of mammals. To functionally characterize the human Grx-TR1 form, we expressed this protein in *E. coli*. Expression constructs were developed that coded for (i) a truncated form terminated at Sec (the Sec-coding UGA codon was intact and terminated translation in the absence of the SECIS element), (ii) a cysteine mutant in which Cys replaced Sec (Sec648Cys), (iii) a wild-type Grx-TR1 [the full sequence was followed by an *E. coli* formate dehydrogenase H SECIS element (*36*)], and (iv) a tagged wild-type enzyme (similar to the wild-type Grx-TR1 form, except that a His tag was cloned at the C-terminus of the enzyme) (Figure 6A). Four corresponding constructs were also developed that lacked the Grx domain. We also separately expressed the Grx domain (Figure 6A).

Table 1: Catalytic Activities of Different Recombinant Grx-TR1 and TR1 Forms in the DTNB Assay

| | truncated form | | cysteine mutant | | wild type | | tagged form | |
|---|---|---|---|---|---|---|---|---|
| | Grx-TR1 | TR1 | Grx-TR1 | TR1 | Grx-TR1 | TR1 | Grx-TR1 | TR1 |
| specific activity (unit/mg) | 0.5 | 0.07 | 0.7 | 0.75 | 0.4 | 0.4 | 0.03 | 0.21 |

All ten recombinant TR1 forms (expressed from four Grx-TR1 constructs, four TR1 module constructs, and two Grx domain constructs) were efficiently expressed in bacteria (Figure 6A). However, in the C-terminally tagged protein, the His tag was located downstream of the Sec-coding TGA. Therefore, only those polypeptides that contained Sec also contained the His tag, and polypeptides that were terminated at the TGA due to low efficiency of Sec insertion into recombinant proteins did not have the His tag. Thus, this construct resulted in a mixture of tagged (~1−10%) and truncated (~90−99%) proteins, but the tagged protein could be separated from the truncated protein using His-tag affinity columns.

Insertion of selenocysteine into the tagged protein was tested by metabolic $^{75}$Se labeling of cells expressing the protein (Figure 6B). Several $^{75}$Se bands were detected (Figure 6B, lane 1 from left), with the major band being the 55 kDa TR1 and others probably being TR1 degradation products and/or proteins nonspecifically labeled with $^{75}$Se. After the affinity purification, only the 55 kDa band remained (Figure 6B, lane 2), which was also stained with anti-His-tag antibodies in immunoblot assays (Figure 6B, lane 3). Since the protein could be labeled with $^{75}$Se and the purified protein contained a His tag downstream of the selenocysteine TGA codon, the data suggested that selenocysteine was indeed inserted into this recombinant TR1 form.

We tested TR activities of the recombinant proteins. With DTNB and NADPH as substrates, the activities of various recombinant TR1 forms (Table 1) were similar to those previously reported (*11*). However, the activities of the recombinant forms of Grx-TR1 showed a different pattern. The truncated form of Grx-TR1 showed higher activity (0.5 unit/mg) than that of truncated TR1 (0.07 unit/mg) while the cysteine mutant of both recombinant forms showed similar activities (0.7 and 0.75 unit/mg). The activities of the cysteine mutant and the truncated form of TR1 were similar to those reported previously (1.15 unit/mg for the cysteine mutant and 0.075 unit/mg for the truncated form, calculated from the original data) (*11*). It is not clear why the truncated form of Grx-TR1 showed higher activity and if it was due to the Grx domain. The His-tagged form of both Grx-TR1 and TR1 showed low activities (0.03 and 0.21 unit/mg), taking into account that these were selenocysteine-containing proteins. A possible explanation is that an extension downstream of the C-terminal active site GCUG (which also included a His tag) blocked the N-terminal thiol/disulfide active site.

The kinetics of the truncated form and the cysteine mutant for the Grx-containing form were determined (Table 2). As previously established (*37*), both forms had similar kinetic parameters. However, in the Trx/insulin assay, all Grx-containing forms were inactive. In contrast, the TR1 forms that lacked the Grx domain (except for the truncated form) exhibited significant activities (0.15 unit/mg for the cysteine mutant, 0.4 unit/mg for the wild type, and 0.2 unit/mg for tagged wild type). The data were consistent with the previous report (*11*) showing that electrons flow through the C-terminal GCUG tetrapeptide and that Cys in place of Sec could partially support the activity.

Table 2: Kinetic Constants of Truncated (Lacks Sec-Gly C-Terminal Dipeptide) and Cysteine Mutant Forms[a]

| | truncated form | cysteine mutant |
|---|---|---|
| $V_{max}$ ($\mu$M/min) | 3.39 | 4.51 |
| $K_m$ (mM) | 0.668 | 1.132 |
| $k_{cat}$ ($min^{-1}$) | 6.28 | 11 |
| $k_{cat}/K_m$ ($min^{-1}\cdot mM^{-1}$) | 9.4 | 9.72 |

[a] Reaction mixtures (0.5 mL) contained 200 $\mu$M recombinant enzymes, 100 mM sodium phosphate buffer, pH 7.0, 0.2 mM NADPH, 10 mM EDTA, and 0.25−5 mM DTNB. Reactions were carried out at 25 °C.

The low activity (0.4 unit/mg) of the recombinant wild-type enzyme was expected. Wild-type TR1 forms expressed in *E. coli* using a bacterial SECIS element incorporate Sec, but the efficiency of Sec insertion is typically low (*38*). Therefore, the isolated N-terminally tagged forms are a mixture of 1−10% full-size and 90−99% truncated proteins. It is difficult to separate full-size and truncated TR forms. In contrast, the isolated C-terminally tagged protein is presumably exclusive in the Sec-containing form, but the presence of the tag appears to interfere with enzyme activity. This observation may provide insight into why the GCUG tetrapeptide is located at the C-terminus of the enzyme. Indeed, further extension of the C-terminal sequence would not be consistent with the reaction mechanism of TR as the C-terminal peptide moves between and shuttles electrons from the CxxxxxC thiol/disulfide center in TR to CxxC in the Trx substrate.

The lack of TR activity (Trx/insulin assay) in Grx-TR1 forms was particularly interesting. As discussed above, the fusion of Grx to the basic TR1 module would place the Grx domain in close proximity of the C-terminal GCUG tetrapeptide, possibly preventing the binding of Trx (*7*). Although the similarly organized TGR exhibits TR activity, it is possible that, in Grx-TR1, a tighter interaction between the fused domains or lower flexibility of the linker peptide between Grx and TR precludes interaction of GCUG and Trx.

To further understand a possible function of the Grx domain, we determined its redox potential by equilibrating the protein with a glutathione buffer, followed by alkylation of reduced cysteines with AMS and analysis of migration properties of oxidized (nonmodified) and reduced (modified and therefore migrating slower) forms using SDS−PAGE (Figure 7). The value of the redox potential was calculated as −210 mV. This value is within the range of redox potentials seen in previously characterized Grxs (−230 mV for Grx1 to −200 mV for Grx3) (*30*) and is also similar to the redox potentials of protein disulfide isomerases (*39*). Thus, the redox potential of the Grx domain is most consistent with its function as either a reductant of a high redox potential substrate or a protein that isomerizes disulfide bonds in substrates.

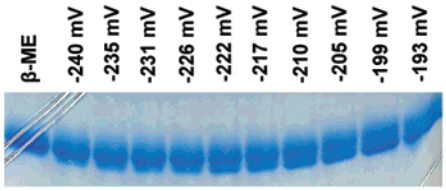


FIGURE 7: Analysis of the redox potential of the Grx domain of human Grx-TR1. The redox potential was determined using a technique described by Regeimbal and Bardwell (*29*). Briefly, a thiol-alkylating compound AMS, which can specifically and irreversibly react with free thiols, was used. The resulting increase in mass of the modified protein (relative to the unmodified protein, in which cysteines are oxidized and are thus not accessible for alkylation) was visualized on an SDS−PAGE gel. Using this technique, the redox status of thiol groups in proteins can be determined and redox potentials calculated when these proteins are incubated in redox buffers with defined redox potentials. The redox potentials of redox buffers were calculated using the Nernst equation as described by Aslund et al. (*30*). The recombinant mutant Grx domain (C3S/C90S) was incubated in buffers containing different ratios of GSH/GSSG (−240 mV, 10 mM GSH/0.1 mM GSSG; −235 mV, 10 mM GSH/0.15 mM GSSG; −231 mV, 10 mM GSH/0.2 mM GSSG; −226 mV, 10 mM GSH/0.3 mM GSSG; −222 mV, 10 mM GSH/0.4 mM GSSG; −217 mV, 10 mM GSH/0.6 mM GSSG; −210 mV, 10 mM GSH/1 mM GSSG; −205 mV, 10 mM GSH/1.5 mM GSSG; −199 mV, 10 mM GSH/2.5 mM GSSG; −193 mV, 5 mM GSH/1 mM GSSG), and the samples were treated with AMS and subjected to SDS−PAGE as indicated in Experimental Procedures. The redox potential of each buffer is indicated above the gel. The upper protein band corresponds to the reduced Grx domain and the lower to oxidized Grx domain. One sample was treated with $\beta$-mercaptoethanol prior to treatment with AMS; it served as control (indicated in the figure as $\beta$-ME).

We further tested the Grx activity of the recombinant Grx domain and found that the Grx domain was inactive in the HED assay. The Grx domain had an unusual CTRC active site instead of the typical CPYC that is found in most Grxs. The residues that separate the two redox cysteines are known to affect redox properties of enzymes (*40*). To test whether the lack of the Grx activity was due to the CTRC motif, we mutated CTRC to CPYC and tested the activity of the mutant protein. The mutated Grx domain, as well as the corresponding Grx-TR1 mutant, exhibited the Grx activity (11 units/mg), although it was somewhat lower compared with other Grxs (*19*).

Since Grx has been reported to also function as dehydroascorbate reductase (*41*), glutathione *S*-transferase (GST) (*42*), peroxidase (*43*), and disulfide isomerase (unpublished data), we tested whether the Grx domain could have any of these activities using either GSH or NADPH as an electron donor. However, the Grx was not active in any of the assays. In addition, we tested the glutathione reductase activity (because TGR is active in glutathione reductase activity assays) but failed to detect activity.

The fact that the Grx-TR1 form was not active in any of the previously established Grx assays and in the Trx assays suggests that this protein has a specific function that is different from those previously reported for either Grx or TR1. The redox potential of the Grx domain is consistent with it being an electron acceptor for the TR1 module. It is possible that Grx-TR1 is a specific reductant for an unknown redox substrate or an enzyme that isomerizes disulfide bonds in testes. In any case, our data differentiate this protein from previously characterized enzymes with fusions between Grx and TR. Indeed, in both mouse TGR and the enzyme isolated from *E. granulosus*, Grx and TR domains could function either in a coupled manner (e.g., transfer of electrons from NADPH to GSSG) or independently of each other (e.g., GSH-dependent HED reduction and NADPH-dependent Trx reduction).

## SUPPORTING INFORMATION AVAILABLE

Table S1 providing detailed information on organization of the human TR1 genes and on alternative splicing forms derived from it, Table S2 illustrating patterns of occurrence of alternative TR1 forms in mammals, Table S3 showing tissue specificity of TR1 forms, Figure S1 showing an alignment of mammalian TR1 promoters, and Figure S2 showing structures of animal TR1 SECIS elements. This material is available free of charge via the Internet at http://pubs.acs.org.

## REFERENCES

1. Arner, E. S., and Holmgren, A. (2000) Physiological functions of thioredoxin and thioredoxin reductase, *Eur. J. Biochem. 267*, 6102−6109.
2. Mustacich, D., and Powis, G. (2000) Thioredoxin reductase, *Biochem. J. 346* (Part 1), 1−8.
3. Holmgren, A. (1980) Pyridine nucleotide−disulfide oxidoreductases, *Experientia, Suppl. 36*, 149−180.
4. Kuriyan, J., Krishna, T. S., Wong, L., Guenther, B., Pahler, A., Williams, C. H., Jr., and Model, P. (1991) Convergent evolution of similar function in two structurally divergent enzymes, *Nature 352*, 172−174.
5. Novoselov, S. V., and Gladyshev, V. N. (2003) Non-animal origin of animal thioredoxin reductases: implications for selenocysteine evolution and evolution of protein function through carboxy-terminal extensions, *Protein Sci. 12*, 372−378.
6. Williams, C. H., Jr. (1995) Mechanism and structure of thioredoxin reductase from *Escherichia coli*, *FASEB J. 9*, 1267−1276.
7. Sun, Q. A., Kirnarsky, L., Sherman, S., and Gladyshev, V. N. (2001) Selenoprotein oxidoreductase with specificity for thioredoxin and glutathione systems, *Proc. Natl. Acad. Sci. U.S.A. 98*, 3673−3678.
8. Arscott, L. D., Gromer, S., Schirmer, R. H., Becker, K., and Williams, C. H., Jr. (1997) The mechanism of thioredoxin reductase from human placenta is similar to the mechanisms of lipoamide dehydrogenase and glutathione reductase and is distinct from the mechanism of thioredoxin reductase from *Escherichia coli*, *Proc. Natl. Acad. Sci. U.S.A. 94*, 3621−3626.
9. Gladyshev, V. N., Jeang, K. T., and Stadtman, T. C. (1996) Selenocysteine, identified as the penultimate C-terminal residue in human T-cell thioredoxin reductase, corresponds to TGA in the human placental gene, *Proc. Natl. Acad. Sci. U.S.A. 93*, 6146−6151.
10. Tamura, T., and Stadtman, T. C. (1996) A new selenoprotein from human lung adenocarcinoma cells: purification, properties, and thioredoxin reductase activity, *Proc. Natl. Acad. Sci. U.S.A. 93*, 1006−1011.
11. Zhong, L., and Holmgren, A. (2000) Essential role of selenium in the catalytic activities of mammalian thioredoxin reductase revealed by characterization of recombinant enzymes with selenocysteine mutations, *J. Biol. Chem. 275*, 18121−18128.
12. Bjornstedt, M., Kumar, S., and Holmgren, A. (1995) Selenite and selenodiglutathione: reactions with thioredoxin systems, *Methods Enzymol. 252*, 209−219.
13. May, J. M., Mendiratta, S., Hill, K. E., and Burk, R. F. (1997) Reduction of dehydroascorbate to ascorbate by the selenoenzyme thioredoxin reductase, *J. Biol. Chem. 272*, 22607−22610.
14. Miranda-Vizuete, A., Damdimopoulos, A. E., Pedrajas, J. R., Gustafsson, J. A., and Spyrou, G. (1999) Human mitochondrial thioredoxin reductase cDNA cloning, expression and genomic organization, *Eur. J. Biochem. 261*, 405−412.
15. Lee, S. R., Kim, J. R., Kwon, K. S., Yoon, H. W., Levine, R. L., Ginsburg, A., and Rhee, S. G. (1999) Molecular cloning and characterization of a mitochondrial selenocysteine-containing thioredoxin reductase from rat liver, *J. Biol. Chem. 274*, 4722−4734.

16. Gasdaska, P. Y., Berggren, M. M., Berry, M. J., and Powis, G. (1999) Cloning, sequencing and functional expression of a novel human thioredoxin reductase, *FEBS Lett. 442*, 105−111.
17. Gromer, S., Wissing, J., Behne, D., Ashman, K., Schirmer, R. H., Flohe, L., and Becker, K. (1998) A hypothesis on the catalytic mechanism of the selenoenzyme thioredoxin reductase, *Biochem. J. 332* (Part 2), 591−592.
18. Zhong, L., Arner, E. S., and Holmgren, A. (2000) Structure and mechanism of mammalian thioredoxin reductase: the active site is a redox-active selenolthiol/selenenylsulfide formed from the conserved cysteine-selenocysteine sequence, *Proc. Natl. Acad. Sci. U.S.A. 97*, 5854−5859.
19. Holmgren, A., and Aslund, F. (1995) Glutaredoxin, *Methods Enzymol. 252*, 283−292.
20. Kanzok, S. M., Fechner, A., Bauer, H., Ulschmid, J. K., Muller, H. M., Botella-Munoz, J., Schneuwly, S., Schirmer, R., and Becker, K. (2001) Substitution of the thioredoxin system for glutathione reductase in *Drosophila melanogaster*, *Science 291*, 643−646.
21. Agorio, A., Chalar, C., Cardozo, S., and Salinas, G. (2003) Alternative mRNAs arising from trans-splicing code for mitochondrial and cytosolic variants of *Echinococcus granulosus* thioredoxin Glutathione reductase, *J. Biol. Chem. 278*, 12920−12928.
22. Alger, H. M., and Williams, D. L. (2002) The disulfide redox system of *Schistosoma mansoni* and the importance of a multifunctional enzyme, thioredoxin glutathione reductase, *Mol. Biochem. Parasitol. 121*, 129−139.
23. Rendon, J. L., del Arenal, I. P., Guevara-Flores, A., Uribe, A., Plancarte, A., and Mendoza-Hernandez, G. (2004) Purification, characterization and kinetic properties of the multifunctional thioredoxin-glutathione reductase from Taenia crassiceps metacestode (cysticerci), *Mol. Biochem. Parasitol. 133*, 61−69.
24. Rundlof, A. K., Carlsten, M., Giacobini, M. M., and Arner, E. S. (2000) Prominent expression of the selenoprotein thioredoxin reductase in the medullary rays of the rat kidney and thioredoxin reductase mRNA variants differing at the 5′ untranslated region, *Biochem. J. 347* (Part 3), 661−668.
25. Sun, Q. A., Zappacosta, F., Factor, V. M., Wirth, P. J., Hatfield, D. L., and Gladyshev, V. N. (2001) Heterogeneity within animal thioredoxin reductases. Evidence for alternative first exon splicing, *J. Biol. Chem. 276*, 3106−3114.
26. Osborne, S. A., and Tonissen, K. F. (2001) Genomic organisation and alternative splicing of mouse and human thioredoxin reductase 1 genes, *BMC Genomics 2*, 10.
27. Kryukov, G. V., Castellano, S., Novoselov, S. V., Lobanov, A. V., Zehtab, O., Guigo, R., and Gladyshev, V. N. (2003) Characterization of mammalian selenoproteomes, *Science 300*, 1439−1443.
28. Thompson, J. D., Higgins, D. G., and Gibson, T. J. (1994) CLUSTAL W: improving the sensitivity of progressive multiple sequence alignment through sequence weighting, position-specific gap penalties and weight matrix choice, *Nucleic Acids Res. 22*, 4673−4680.
29. Regeimbal, J., and Bardwell, J. C. (2002) DsbB catalyzes disulfide bond formation de novo, *J. Biol. Chem. 277*, 32706−32713.
30. Aslund, F., Berndt, K. D., and Holmgren, A. (1997) Redox potentials of glutaredoxins and other thiol-disulfide oxidoreductases of the thioredoxin superfamily determined by direct protein−protein redox equilibria, *J. Biol. Chem. 272*, 30780−30786.
31. Arner, E. S., Zhong, L., and Holmgren, A. (1999) Preparation and assay of mammalian thioredoxin and thioredoxin reductase, *Methods Enzymol. 300*, 226−239.
32. Smith, I. K., Vierheller, T. L., and Thorne, C. A. (1988) Assay of glutathione reductase in crude tissue homogenates using 5,5′-dithiobis(2-nitrobenzoic acid), *Anal. Biochem. 175*, 408−413.
33. Woycechowsky, K. J., and Raines, R. T. (2003) The CXC motif: a functional mimic of protein disulfide isomerase, *Biochemistry 42*, 5387−5394.
34. Jurado, J., Prieto-Alamo, M. J., Madrid-Risquez, J., and Pueyo, C. (2003) Absolute gene expression patterns of thioredoxin and glutaredoxin redox systems in mouse, *J. Biol. Chem. 278*, 45546−45554.
35. Rundlof, A. K., Carlsten, M., and Arner, E. S. (2001) The core promoter of human thioredoxin reductase 1: cloning, transcriptional activity, and Oct-1, Sp1, and Sp3 binding reveal a housekeeping-type promoter for the AU-rich element-regulated gene, *J. Biol. Chem. 276*, 30542−30551.
36. Arner, E. S., Sarioglu, H., Lottspeich, F., Holmgren, A., and Bock, A. (1999) High-level expression in *Escherichia coli* of selenocysteine-containing rat thioredoxin reductase utilizing gene fusions with engineered bacterial-type SECIS elements and co-expression with the selA, selB and selC genes, *J. Mol. Biol. 292*, 1003−1016.
37. Gilberger, T. W., Bergmann, B., Walter, R. D., and Muller, S. (1998) The role of the C-terminus for catalysis of the large thioredoxin reductase from *Plasmodium falciparum*, *FEBS Lett. 425*, 407−410.
38. Arner, E. S. (2002) Recombinant expression of mammalian selenocysteine-containing thioredoxin reductase and other selenoproteins in *Escherichia coli*, *Methods Enzymol. 347*, 226−235.
39. Sevier, C. S., and Kaiser, C. A. (2002) Formation and transfer of disulphide bonds in living cells, *Nat. Rev. Mol. Cell Biol. 3*, 836−847.
40. Chivers, P. T., Prehoda, K. E., and Raines, R. T. (1997) The CXXC motif: a rheostat in the active site, *Biochemistry 36*, 4061−4066.
41. Wells, W. W., Xu, D. P., Yang, Y. F., and Rocque, P. A. (1990) Mammalian thioltransferase (glutaredoxin) and protein disulfide isomerase have dehydroascorbate reductase activity, *J. Biol. Chem. 265*, 15361−15364.
42. Collinson, E. J., and Grant, C. M. (2003) Role of yeast glutaredoxins as glutathione S-transferases, *J. Biol. Chem. 278*, 22492−22497.
43. Collinson, E. J., Wheeler, G. L., Garrido, E. O., Avery, A. M., Avery, S. V., and Grant, C. M. (2002) The yeast glutaredoxins are active as glutathione peroxidases, *J. Biol. Chem. 277*, 16712−16717.

BI048478T